ELSEVIER

Bone 37 (2005) 159 – 169

BONE

www.elsevier.com/locate/bone

Response to continuous and pulsatile PTH dosing: A mathematical model for parathyroid hormone receptor kinetics

Laura K. Potter[a,*], Larry D. Greller[b,1], Carolyn R. Cho[b,1], Mark E. Nuttall[c,2], George B. Stroup[c], Larry J. Suva[d,3], Frank L. Tobin[e]

[a]*Scientific Computing and Mathematical Modeling, GlaxoSmithKline, Research Triangle Park, NC, USA*
[b]*Bioinformatics, GlaxoSmithKline, King of Prussia, PA, USA*
[c]*Musculoskeletal Diseases Biology Section, GlaxoSmithKline, King of Prussia, PA, USA*
[d]*Bone and Cartilage Biology, GlaxoSmithKline, King of Prussia, PA, USA*
[e]*Scientific Computing and Mathematical Modeling, GlaxoSmithKline, King of Prussia, PA, USA*

Received 20 December 2004; revised 23 March 2005; accepted 5 April 2005
Available online 25 May 2005

Abstract

In this paper, we propose a mathematical model for parathyroid hormone receptor (PTH1R) kinetics, focusing on the receptor's response to PTH dosing to discern bone formation responses from bone resorption. The PTH1R is a major target for new osteoporosis treatments, as pulsatile PTH dosing has been shown to induce net bone formation in both animals and humans, and PTH(1–34) was recently FDA approved for the treatment of post-menopausal osteoporosis. PTH has also been shown to cause net bone loss when given continuously, so that the net action of PTH on bone is dependent on the dosing pattern. We have developed a simplified two-state receptor kinetics model for the PTH1R, based on the concepts of Segel et al., to distinguish the activity of active and inactive receptor and receptor–ligand complexes. The goal is to develop a plausible model of the minimal essential biological relationships necessary for understanding the responses to PTH dosing. A two-state model is able to effectively discriminate between continuous and pulsatile PTH dosing using the active species as surrogates for the downstream anabolic response. For continuous PTH dosing, the model predicts a desensitized system dominated by the inactive receptor and complex, consistent with downstream net bone loss that has been demonstrated experimentally. Using pulsatile PTH dosing, the model system predicts a highly sensitized state dominated by the active receptor and complex, corresponding to net bone formation. These results are consistent with the hypothesis that the kinetics of the receptor plays a critical role in the downstream effects of PTH dosing. Moreover, these results indicate that within a range of biologically relevant PTH doses, the two-state model is able to capture the differential behavior of the system for both continuous and pulsatile PTH dosing. The development of such a model provides a rational basis for developing more biologically extensive models that may support the design of optimal dosing strategies for PTH-based anti-osteoporosis treatments. Moreover, this model provides a unique starting point from which to design experiments investigating PTH receptor biology.

Keywords: Parathyroid hormone; Parathyroid hormone receptor; Mathematical model; Osteoporosis; Receptor kinetics

Introduction

Pulsatile administration of parathyroid hormone (PTH) has been shown to have a strong anabolic effect on bone in both animals and humans [1–5]. As a result, the PTH signaling pathway is considered a promising target for the development of new anabolic treatments for osteoporosis. This pathway involves the binding of PTH to the PTH Type 1 receptor (PTH1R) in osteoblastic target cells, leading to

* Corresponding author.
E-mail address: laura.k.potter@gsk.com (L.K. Potter).
[1] Current address: Biosystemix Ltd., Kingston, ON, Canada.
[2] Current address: Centocor, Malvern, PA, USA.
[3] Current address: Department of Orthopaedic Surgery, Center for Orthopedic Research, Univ. of Arkansas for Medical Sciences, Little Rock, AR, USA.

8756-3282/$ - see front matter © 2005 Elsevier Inc. All rights reserved.
doi:10.1016/j.bone.2005.04.011

signal transduction cascades that influence bone turnover [6]. Compounds that act as PTH1R agonists have potential for development as osteoporosis therapies. The truncated peptide PTH(1–34), available under the generic name teriparatide, is currently the only marketed anabolic therapy for osteoporosis [5].

A major difficulty with this therapeutic approach arises from the paradigm of PTH action, namely that continuous PTH administration is catabolic to the skeleton, resulting in increased osteoclastic bone resorption [7,8], whereas pulsatile doses of PTH result in net bone formation [7,9,10]. Despite many attempts to identify the source of these differential dosing effects on bone turnover, the precise mechanism remains elusive [11–15].

The PTH-mediated signaling pathway in osteoblasts is a complicated network that stems from the interaction of ligand-bound PTH1R and two distinct G proteins [6]. Although numerous studies have explored many of the components of the PTH signal transduction pathway [7,16–20], much of the pathway has yet to be detailed. This lack of sufficient detail adds to the difficulty in determining the specific mechanism(s) for the differential effects of PTH dosing on the skeleton.

To effectively utilize the PTH1R signaling pathway for potential osteoporosis therapies, it is crucial to understand the dynamics of PTH binding and signal transduction. A major unresolved question is how the dynamic response of the PTH1R receptor is related to PTH action on bone and to the differential effects of continuous versus pulsatile PTH dosing. One hypothesis is that PTH1R kinetics is central to the differential response to distinct dosing patterns. If this hypothesis is correct, it may be possible to simplify the prediction of the downstream effects of PTH and other PTH1R agonists on bone formation based on the interaction of these compounds solely with the PTH1R system. Hence, the model described here focuses only on the dynamics of the PTH1R.

Determining the kinetics of the receptor would have major implications for further studies to determine the exact mechanism(s) by which both pulsatile and continuous PTH dosing impact bone. If the differential response to the two dosing patterns occurs as early as the receptor itself, it suggests that experimental exploration of the dynamics of PTH1R binding, activation/inactivation, and early signaling would be informative.

Conversely, if the receptor kinetics are not crucial to the differential response, then it may be more prudent to focus experimental efforts on longer-term, downstream signaling responses. Other hypotheses for explaining the differential response to different dosing patterns are focused on downstream signal transduction. Locklin et al. [21] suggest that continuous PTH dosing increases osteoclast numbers via the RANKL pathway, while pulsatile dosing stimulates osteoblast differentiation but not the RANKL pathway. Qin et al. [22] propose that negative feedback loops in the PTH1R-mediated signaling networks lead to long-term desensitization of signal when dosing is continuous, while pulsatile doses achieve more signaling over time because the system resensitizes between doses.

A mathematical model has been developed for PTH1R kinetics to explore the hypothesis that the dynamics of the receptor are central to the differential response to continuous vs. pulsatile PTH dosing. The objective was to build a biologically plausible model that captures only the essential features of PTH1R activation but exhibits known behaviors such as receptor desensitization and resensitization [23]. The resulting model was tested to determine if the response of such a system could distinguish between continuous and pulsatile PTH administration. Although it is not feasible to monitor the full breadth of PTH1R dynamics experimentally, the model can be used as a mechanistic basis to support the idea that the kinetics of PTH1R plays an important role in the downstream response to PTH dosing.

Other mathematical models have been developed that incorporate the larger-scale, downstream effects of PTH on the bone remodeling cycle. Kroll [24] built a model that describes PTH stimulation and inhibition of osteoblast and osteoclast differentiation and proliferation, and Rattanakul et al. [25] have a somewhat simpler model for the effects of PTH on osteoblast and osteoclast numbers. These models do not directly incorporate the dynamics of PTH1R binding and signal transduction, but instead are able to qualitatively reproduce the large-scale effects of continuous vs. pulsatile PTH on osteoblasts and osteoclasts without explaining the precise mechanism. Lemaire et al. [26] incorporate more detailed biology in a model for the remodeling cycle that includes the effects of PTH on osteoclasts but not the formation-stimulating effects on osteoblasts.

In this study, a minimal mathematical model for PTH1R kinetics is presented. The model and its function as a highly nonlinear dosing transducer are based on a standard "two-state" receptor desensitization/adaptation model of Segel et al. [27]. Simulations representing different PTH dosing regimens suggest that the model is biologically relevant and capable of discriminating pulsatile vs. continuous PTH dosing. These results are entirely consistent with the hypothesis that PTH1R kinetics is important in mediating PTH effects on the skeleton.

Bone remodeling and PTH signaling

Bone remodeling is largely a localized phenomenon that occurs at the level of a basic multicellular unit (BMU) [28], consisting primarily of the action of osteoclasts and osteoblasts. The bone remodeling cycle consists of three stages: activation of the remodeling site, resorption of bone by the osteoclasts, and bone formation by the osteoblasts.

This cycle is under the control of several systemic hormones and local factors. Parathyroid hormone (PTH), naturally secreted by the parathyroid glands in a pulsatile pattern of about seven bursts per hour, is involved (along with vitamin D) in the regulation of serum calcium [29].

PTH acts directly on osteoblasts via binding to PTH1R to promote bone formation.

The effects of PTH on bone are mediated by the binding of PTH to the PTH1R, a G protein-coupled seven transmembrane receptor that interacts separately with the G_s and G_q proteins. PTH1R, like many other G protein-coupled receptors, is subject to desensitization following prolonged or repeated exposure to its ligand [30–34]. After an initial increase in ligand-mediated signaling, the continued and/or repeated presence of the ligand leads to a decrease in signaling that returns to original levels only after a sufficient "resensitization" period where little or no ligand is present [23]. Several mechanisms including receptor phosphorylation, G protein uncoupling from the receptor complex, and internalization of the receptor have been proposed for receptor desensitization [31–33,35].

An association between the desensitization of PTH1R signaling and the resulting net change in bone mass has been proposed to explain the differential response in signaling to the continuous and pulsatile presence of ligand [31,34]. This idea motivated the implementation of this model for PTH1R kinetics.

Model development

Receptor kinetics models have been developed for many different receptor systems, ranging from general models for entire classes of receptors to specific models for a particular receptor expressed in a specific cell type (see [36,37] for reviews of existing models). G protein-coupled receptors (GPCRs), such as the PTH1R, are known to exist in various conformations that have different affinities for processes such as binding, activation, and phosphorylation [38,39]. It has been shown that PTH1R undergoes multiple conformational changes as it binds to ligands and becomes activated [11,40]. We conceptually group these multiple conformations in two functional states: active and inactive.

A widely accepted model for the activation of GPCRs is the "two-state" model (e.g., see [27,37,41,42]) based on the assumption that the receptor exists in two distinct functional states: an active R_a and an inactive R_i. It is further assumed that the receptor can switch between these two states, regardless of its binding to its ligand, based on the ability of PTH1R to change conformation independent of ligand. This leads to the corresponding active and inactive states of the ligand–receptor complex, denoted here as C_a and C_i, respectively (see Fig. 1 for a schematic of the model kinetics).

The two-state model is a good candidate for modeling the dynamics of different PTH dosing response patterns, since it distinguishes between active and inactive receptor and ligand–receptor complexes [41]. In the case of the PTH1R, the active complex can be interpreted as the G protein-coupled, PTH-bound receptor, with the inactive complex representing PTH-bound receptor that is not coupled to a G protein [43]. Similarly, the active and inactive receptor species can be interpreted as G protein-coupled receptor and uncoupled receptor, respectively [43]. Although the two-state model significantly simplifies the overall dynamics of the receptor, it can encompass much of the biology of a GPCR such as the PTH1R.

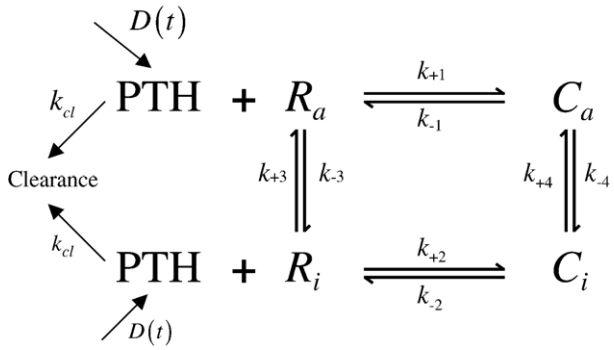

Fig. 1. Two-state model for PTHR1 binding kinetics. PTH is secreted and/or dosed at rate $D(t)$ as given in (2). The active and inactive forms of the receptor, denoted as R_a and R_i, respectively, are available to bind with PTH to form the corresponding active and inactive complexes C_a and C_i. In addition, there is a conversion between the inactive and active forms of the receptor and complexes, while unbound PTH is cleared from the system. Rate constants are detailed in Table 1.

The mathematical basis for the PTH receptor model is the well-described (e.g., [36,44]) model of Segel et al. [27]. This scheme provides a plausible explanatory kinetics mechanism for the phenomenon of "exact adaptation" of receptors to stimuli. In so-called exact or partial adaptation, a receptor-mediated biological response more or less reverts through time to the biological system's basal response level when in the presence of *sustained quasi-steady stimuli*, which are stimuli that are constant or near-constant in time [27]. An example of an "adapting" system discussed in [27] involves desensitization of intracellular cAMP synthesis in the cellular slime mold *Dictyostelium discoideum*.

The "adaptation" of system responses to a sustained steady stimulus is often independent of the stimulus level. Whereas, time-varying responses (which are at levels elevated substantially above the basal, such as pulsatile PTH) are elicited by *time-varying stimuli*—and are often very sensitive to those stimuli. These dependencies vary with stimulus frequency, amplitude, and the characteristic sensitization and desensitization times of the ligand–receptor on- and off-rates and the bound-species conversion rates [27].

Here, the model is employed as a plausible kinetics scheme for PTH1R that behaves essentially as an appropriate temporal signal nonlinear filter that supplies an effective dynamical molecular discrimination of pulsatile from steady-state dosing of PTH. Employment of the model scheme in this fashion for input signal discrimination has precedent and is in the spirit of Goldbeter [44].

In the study described herein, the binding kinetics of the two-state model together with the endogenous secretion

and/or dosing of PTH and the clearance of unbound PTH was used to obtain the following system of mass–action, mass–balance equations (see Fig. 1):

$$\frac{dP}{dt} = k_{-1}C_a + k_{-2}C_i - k_{+1}R_aP - k_{+2}R_iP - k_{cl}P + D(t)$$

$$\frac{dR_a}{dt} = k_{-1}C_a + k_{+3}R_i - k_{+1}R_aP - k_{-3}R_a$$

$$\frac{dR_i}{dt} = k_{-2}C_i + k_{-3}R_a - k_{+2}R_iP - k_{+3}R_i$$

$$\frac{dC_a}{dt} = k_{+1}R_aP + k_{+4}C_i - k_{-1}C_a - k_{-4}C_a$$

$$\frac{dC_i}{dt} = k_{+2}R_iP + k_{-4}C_a - k_{-2}C_i - k_{+4}C_i, \quad (1)$$

where P denotes the concentration of PTH and R_a, R_i, C_a, C_i denote the concentrations of the corresponding active and inactive receptors and complexes. All concentrations are in pM. The forcing function, $D(t)$, represents the PTH dosing (in pM/s) and is given by

$$D(t) = D_e(t) + D_d(t), \quad (2)$$

where $D_e(t)$ represents the endogenous secretion flux of PTH and $D_d(t)$ represents external PTH dosing. Model parameters k_{cl}, k_{+1}, k_{+2}, k_{-1}, k_{-2}, k_{+3}, k_{-3}, k_{+4}, k_{-4} are summarized in Table 1.

The equilibrium dissociation constant K_D is given as the ratio of the ligand–receptor binding dissociation rate k_{off} (e.g., the model parameters k_{-1}, k_{-2}) and the binding association rate k_{on} (e.g., the model parameters k_{+1}, k_{+2}), so that $K_D = k_{off}/k_{on}$ [45]. Measured values of K_D for PTH in the literature range from approximately 0.1 to 1 nM [16,46–48]. Here, we assume that the majority of PTH1R is in the active form R_a, so that the equilibrium dissociation constant K_{D_1} is equal to the overall K_D, with $K_{D_1} = 1$ nM $= 10^3$ pM. Moreover, we assume the relationship

$$K_{D_1} = \beta K_{D_2},$$

where β is the "conformational selectivity" parameter [49], and represents the difference in binding activity between the inactive and active species. In this case, we assume that $\beta = 0.1$, so that $K_{D_2} = 10^4$ pM.

To estimate the binding association rates k_{+1} and k_{+2}, the equilibrium constants K_{D_1} and K_{D_2} are used together with the assumption that the dissociation rates k_{-1} and k_{-2} of the ligand–receptor complexes are equal to 10^{-3} s^{-1} so that

$$k_{+1} = \frac{k_{-1}}{K_{D_1}} = 10^{-6}\text{pM}^{-1}\text{s}^{-1},$$

$$k_{+2} = \frac{k_{-2}}{K_{D_2}} = 10^{-7}\text{pM}^{-1}\text{s}^{-1}.$$

The rates k_{+3} and k_{-3} for the conversion of the unbound receptor species R_a and R_i are more difficult to determine. As we were unable to find measurements of conversion rates between active and inactive forms of PTH1R in the literature, the values for k_{+3} and k_{-3} were selected based on modification rates for the cAMP receptor in *Dictyostelium discoideum* [44]. Although the corresponding rates for the human PTH1R are likely to have different values, the rates determined by Goldbeter [44] provide biologically relevant parameters that can be used to test the behavior of the two-state model. In fact, if the two-state model is able to qualitatively reproduce the differential responses to continuous and pulsatile PTH dosing, future efforts will focus on building a more biologically sophisticated model with parameters based on PTH1R-specific experimental data.

The assumption is made that the modification rate, k_{+3}, for $R_i \rightarrow R_a$ is similar in magnitude to the dissociation rate k_{-1} for the active receptor–ligand complex C_a. In particular, we set $k_{+3} = k_{-1} = 10^{-3}$ s^{-1}. Moreover, we utilize the assumption from [44] that

$$k_{-3} = \frac{k_{+3}}{10} = 10^{-4}\text{s}^{-1}.$$

The conversion rates, k_{+4} and k_{-4}, for the PTH-bound receptor complex were based on qualitative information about PTH1R binding as well as rates for the cAMP receptor in [44]. While the conversion rate k_{+4} has not been directly measured, there is evidence suggesting that the tendency to convert from the inactive to the active state is stronger for the ligand–bound receptor complex than for the unbound receptor [50]. Here, we assume that the conversion rate k_{+4} is twice the conversion rate of the unbound receptor, so that

$$k_{+4} = 2k_{+3} = 2 \times 10^{-3}\text{s}^{-1}.$$

Table 1
Parameter values for the two-state model (1) as illustrated in Fig. 1

Parameter	Rate constant description	Value	Source
k_{+1}	PTH binding to R_a	10^{-6} s^{-1} pM^{-1}	Calculated from K_{D_1}
k_{-1}	C_a dissociation	10^{-3} s^{-1}	Assumption
k_{+2}	PTH binding to R_i	10^{-7} s^{-1} pM^{-1}	Calculated from K_{D_2}
k_{-2}	C_i dissociation	10^{-3} s^{-1}	Assumption
k_{+3}	Conversion of $R_i \rightarrow R_a$	10^{-3} s^{-1}	Assumption
k_{-3}	Conversion of $R_a \rightarrow R_i$	10^{-4} s^{-1}	Calculation based on [44]
k_{+4}	Conversion rate for $C_i \rightarrow C_a$	2×10^{-3} s^{-1}	Calculation based on [44]
k_{-4}	Conversion rate for $C_a \rightarrow C_i$	0.4 s^{-1}	Calculation based on [44]
k_{cl}	Clearance rate for PTH	5×10^{-3} s^{-1}	Literature [51,52]

Details on derivation of parameter values are given in the text.

The value for k_{-4} is then determined using another assumption from [44]:

$$k_{-4} = \frac{k_{+4}}{0.005} = 0.4\text{s}^{-1}.$$

Finally, the clearance rate k_{cl} for PTH is estimated as 5×10^{-3} s^{-1}, which is based on experimental data demonstrating that the approximate half-life of PTH is approximately 2 min [51,52]. The total concentration of receptor, given by

$$R_{tot} = R_a + R_i + C_a + C_i,$$

is estimated as 10 pM. This assumes approximately 10^4 receptors per osteoblastic cell with a cellular density of 10^6 cells/ml (an estimate of the cell density of soft tissue). The measurement of osteoblastic PTH1R number is entirely consistent with the available experimental evidence [53].

The effects of different PTH dosing patterns may be explored by altering the form of the forcing function $D_d(t)$. Both continuous and pulsatile dosing can be represented in the following general form:

$$D_d(t) = \begin{cases} d_{\max} & \text{if } t \in \left[(j-1)(\tau_{on}+\tau_{off}), j\tau_{on}+(j-1)\tau_{off}\right] \\ d_{\min} & \text{if } t \in \left[j\tau_{on}+(j-1)\tau_{off}, j(\tau_{on}+\tau_{off})\right] \end{cases} \quad (3)$$

for $j = 1,\ldots, N$, where $N(\tau_{on} + \tau_{off})$ is equal to the maximum time t_f of the entire dosing experiment. See Fig. 2 for a graph of D_d versus time. The parameters τ_{on} and τ_{off} represent the amount of time that the dose level is set to d_{max} and d_{min} pM/s, respectively.

For continuous dosing, set $\tau_{on} = t_f, \tau_{off} = 0$, with d_{max} set at the appropriate constant dosing rate. Pulsatile dosing is achieved using positive values of τ_{on} and τ_{off} with $d_{min} = 0$. A bolus dose at time zero can be approximated by setting the initial concentration of PTH to the amount of the dose and $D_d(t) = 0$ for all t. Note that the dosing function $D_d(t)$ also can be generalized to incorporate the pharmacokinetics of a compound using standard sums of exponentials.

For in vivo systems with intact parathyroid function, the endogenous secretion of PTH from the parathyroid gland must be considered. The secretion of PTH from the parathyroid gland is highly pulsatile, with approximately seven secretory bursts per hour in adult humans [51,52].

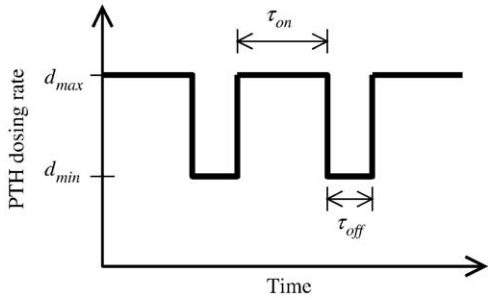

Fig. 2. General PTH dosing function $D_d(t)$ as given in (3). By adjusting the parameters τ_{on} and τ_{off}, the dosing pattern can range from continuous dosing ($\tau_{off} = 0$) to pulsatile dosing ($\tau_{on} \approx 0$, $d_{min} = 0$).

Baseline secretion is responsible for roughly 60–70% of the total PTH secretion, with mean plasma PTH concentrations maintained around 3 pM [51,52,54]. Therefore the endogenous secretion function $D_e(t)$ must capture both baseline and pulsatile secretion. For the majority of this paper, we will focus on dosing studies for ex vivo systems with no endogenous PTH secretion, so that $D_e(t) \equiv 0$.

Segel et al. [27] examined the behavior of the two-state model during initial fast transient periods and at asymptotic steady-states. In the case of a constant forcing function, it is easily seen that the model is driven to a stable equilibrium. Since the goal is to use the two-state model (1) to test the idea that a simple receptor kinetics model can discriminate between different PTH dosing patterns, a discussion of model stability is omitted. This model, if capable of distinguishing between distinct dosing patterns, will serve as the core for an expanded, more biologically detailed model of PTH dynamics. Rather than focus efforts on theoretical results for the "test" model (1), we will defer a formal stability analysis to the more detailed PTH kinetics model.

Results

The effects of different PTH dosing regimens on the receptor and complex concentrations were explored using the general dosing function $D_d(t)$ given in (3). We used a stiff ODE solver [55] to solve numerically the model equations (1) with the parameter values given in Table 1. This type of solver is used to handle systems where the dynamic behavior of one or more variables occurs on a significantly different time scale than the others, and is also effective at solving general non-stiff systems [55]. Depending on the model parameter values, the two-state model has the potential to exhibit both stiff and non-stiff behavior.

First the response of the system to different levels of continuous PTH dosing was studied. A "low-dose" state was obtained by driving the model to equilibrium with the dosing function

$$D_d(t) \equiv 0.015\text{pM/s},$$

which yields a constant PTH concentration of 3 pM, a value that approximates the plasma concentration of PTH in humans [51,52,54]. In the same manner a "high-dose" state was obtained with $D_d(t) \equiv 7.5$ pM/s, which results in a constant concentration of 1500 pM PTH. Steady-state values for the low-dose and high-dose equilibria are given in Table 2. To quantify the difference between these two states, we define the fraction of receptors in the active state as the following measure of sensitization:

$$\rho = \frac{R_a + C_a}{R_a + C_a + R_i + C_i}. \quad (4)$$

As seen in Table 2, the low-dose equilibrium is highly sensitized ($\rho = 0.90$) compared to the high-dose equilibrium

Table 2
Comparison of low-dose and high-dose equilibria for the two-state model (1)

Variable	Value at low-dose equilibrium	Value at high-dose equilibrium
P	3	1500
R_a	16.9	4.3
R_i	1.7	6.8
C_a	4e−4	0.05
C_i	0.05	7.4
ρ	0.90	0.23

The low-dose equilibrium was obtained by driving the system to steady-state with the dosing function $D_d(t) = 0.015$ pM/s, while the high-dose equilibrium was obtained in the same manner with $D_d(t) = 7.5$ pM/s. The concentrations P, R_a, R_i, C_a, C_i are given in pM. The dimensionless variable ρ represents the proportion of active receptor and complex as in (4), and is a measure of the sensitization of the system. Note that the low-dose state is significantly more sensitized than the high-dose state.

($\rho = 0.23$). The dynamics of the desensitization that occur as the model is driven from the low-dose state to the high-dose state are given in Fig. 3; note the pronounced decrease of active receptor R_a and concurrent increase of inactive complex C_i. The characteristic response time of desensitization, which is measured as the time required for ρ to reach the desensitized steady-state, is approximately 36 min. This number is similar to the reported time of 30 min for PTH1R-mediated cAMP desensitization [56] and complete internalization of PTH1R [33].

System resensitization occurs as the system is driven from the high-dose state to the low-dose state (see Fig. 3). The characteristic response time of resensitization is approximately 104 min, which is comparable to the reported times of 2 h for PTH1R resensitization [23] and 1–2 h for complete PTH1R recycling back to the plasma membrane [33].

The characteristic response times for desensitization and resensitization are largely dependent on the scale of the model parameters. In particular, by scaling equally all of the rate constants for binding, dissociation and conversion (i.e., all parameters except for the PTH clearance rate k_{cl}), the characteristic response times are scaled in the opposite direction. Significant sensitivity of these response times to individual parameters occurred only for the binding rates k_{+1}, k_{+2} and dissociation rate k_{-2}.

The sensitivity of the sensitized and desensitized states ρ to the model parameters was also explored. Fig. 4 illustrates the percent change in the sensitized and desensitized states (summarized by ρ) in response to a ±50% change in individual model parameters. The receptor conversion rates k_{+3}, k_{-3} exhibit the greatest sensitivity for the sensitized state, while the desensitized state has significant sensitivity to the PTH clearance rate k_{cl} and the rate constants k_{+1}, k_{+3}, and k_{-2}. Since the main objective of this effort was only to develop a plausible model that can discriminate between different dosing patterns, a more formal sensitivity study and stability analysis is deferred to a future, more biologically detailed model that is specific to the PTH1R.

The dynamics of pulsatile PTH dosing were explored and, as previously discussed, high continuous dose levels of PTH drive the system to a desensitized state, whereas low doses of PTH lead to a sensitized state. With pulsatile dosing, the system oscillates between the sensitized and desensitized states dependent on the dose level and the on and off times τ_{on} and τ_{off}. For example, the initially sensitized system is driven to a lower sensitization state when the high dose level (7.5 pM/s) is used with $\tau_{on} = \tau_{off} = 0.5$ h, as seen in Fig. 5. This is because the characteristic response time for resensitization is longer than the response time for desensitization, such that net desensitization occurs. Using a τ_{off} greater than the characteristic resensitization response time of 104 min would allow for resensitization after each dose.

Since the system sensitization, ρ, oscillates when the dosing pattern is periodic, we need an additional measure to quantify the long-term sensitization for pulsatile dosing. We define $\bar{\rho}$ as the mean of ρ over one period of the dosing function $D_d(t)$ when the system has been driven to homeostasis.

To validate the ability of $\bar{\rho}$ to compare the long-term system sensitization for different dosing patterns, the model was tested for the limiting cases of pulsatile and continuous

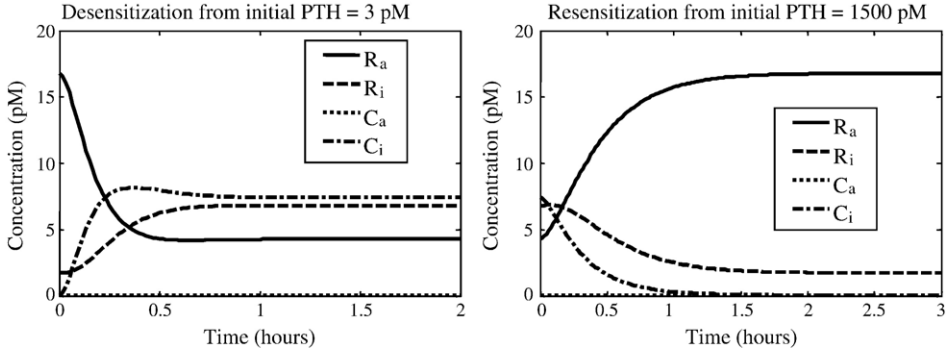

Fig. 3. PTH1R kinetics. Desensitization (left) and resensitization (right) of active receptor R_a and active complex C_a in response to PTH dosing. For desensitization, the initial conditions correspond to the sensitized state as in Table 2. The PTH dose is then increased by setting $D_d(t) = 7.5$ pM/s for all t, which produces a new equilibrium state with a constant concentration of 1500 pM PTH as in Table 2. For resensitization, the model is driven from the desensitized, high-dose equilibrium back to the sensitized state using a PTH-dosing function of $D_d(t) = 0.015$ pM/s for all times.

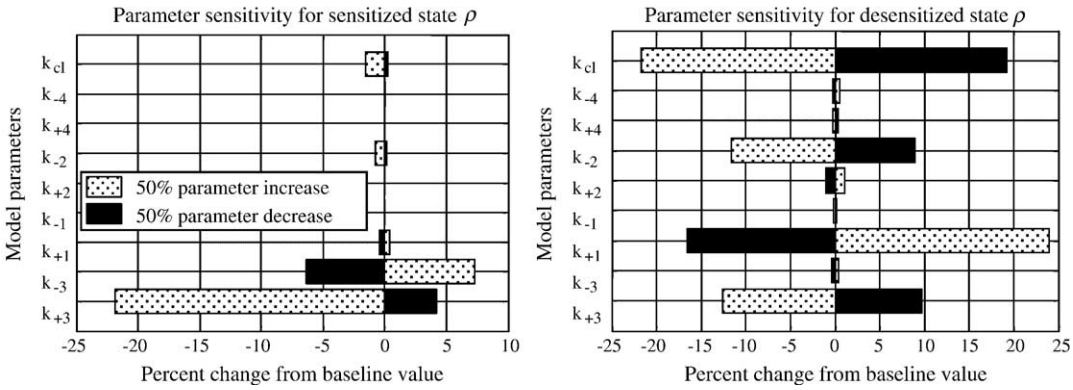

Fig. 4. Sensitivity of sensitized (left) and desensitized (right) states ρ to individual model parameters. The model was driven from the sensitized/desensitized states (respectively) to a new steady-state with a ±50% change in a single model parameter, and the percent change in ρ is given above.

dosing. When a high PTH dose is delivered in a nearly-constant pattern to the initially sensitized state, the dynamics in ρ correspond well with those for the same dose given continuously, with $\bar{\rho} = 0.25$ for both cases. Similarly, when starting from the desensitized state, a dosing pattern with high, short pulses of PTH compares with a low continuous dose of PTH, with $\bar{\rho} = 0.90$ in both cases. These results suggest that $\bar{\rho}$ is a feasible measure of long-term sensitization for comparing dosing patterns, and that the square wave dosing function (3) is able to capture the limiting behaviors of continuous and pulsatile dosing.

Using the general dosing function (3), we studied the effects of a high PTH dose (7.5 pM/s) on the initially sensitized system for varying on and off-times τ_{on} and τ_{off}. The on and off-times ranged from 10 min to 24 h, and for each pair (τ_{on}, τ_{off}) the resulting long-term sensitization $\bar{\rho}$ is shown in Fig. 6, with light shades representing high sensitization and dark shades representing low sensitization.

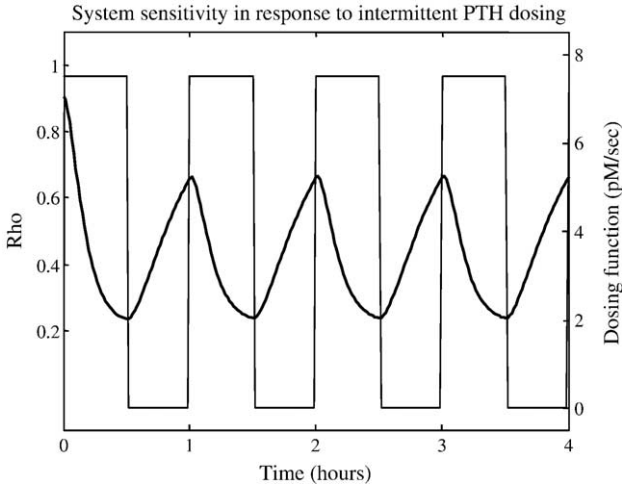

Fig. 5. System sensitization ρ (thick line) of the two-state model (1) in response to pulsatile PTH dosing (thin line). The initial conditions for the simulation correspond to the low-dose equilibrium as in Table 2, and the dosing function (3) was used with $d_{max} = 7.5$ pM/s (corresponding to the high-dose scenario) and $\tau_{on} = \tau_{off} = 0.5$ h. After the first hour, the system is significantly desensitized since the off-time τ_{off} is insufficient to allow for full resensitization.

As seen in Fig. 6, the system has the greatest long-term sensitization $\bar{\rho}$ for small on-times and large off-times. This is consistent with the observation that high continuous dosing leads to desensitization as characterized by small values of $\bar{\rho} = \rho$, while pulsatile dosing results in resensitization and larger $\bar{\rho}$. This suggests that the two-state model (1) is able to successfully discriminate between continuous and pulsatile PTH dosing, with pulsatile dosing resulting in higher sensitization and thereby potential activity.

The ability of the model to discriminate between continuous and pulsatile dosing may vary with different dose levels and/or receptor concentrations. The behavior of the model for a range of receptor concentrations and PTH dosing levels was tested. As seen in Fig. 7, the model is able to discriminate between continuous and pulsatile dosing for all concentrations of receptor tested (0.1 to 2500 pM), given

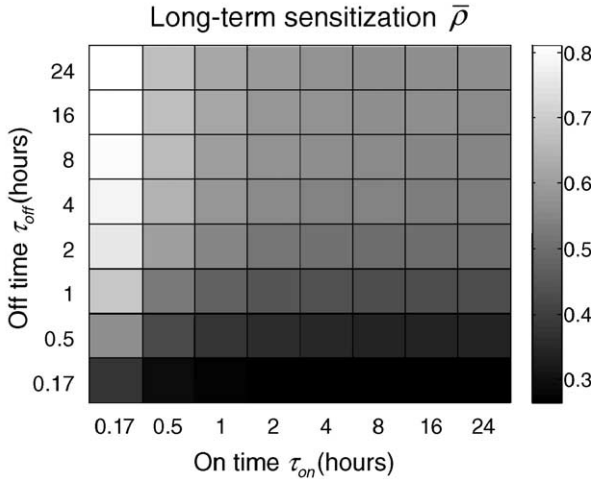

Fig. 6. Long-term sensitization $\bar{\rho}$ for a range of pulsatile dosing patterns. The initial conditions correspond to the sensitized, low-dose continuous state as in Table 2. The dosing function (3) was used for varying on and off times τ_{on} and τ_{off} with $d_{max} = 7.5$ pM/s, and the resulting long-term sensitizations $\bar{\rho}$ are given in the figure with values corresponding to those given in the colorbar. The long-term sensitization is highest for small on times and large off times (approximating pulsatile dosing), while sensitization is lowest for large on times and small off times (approximating continuous dosing).

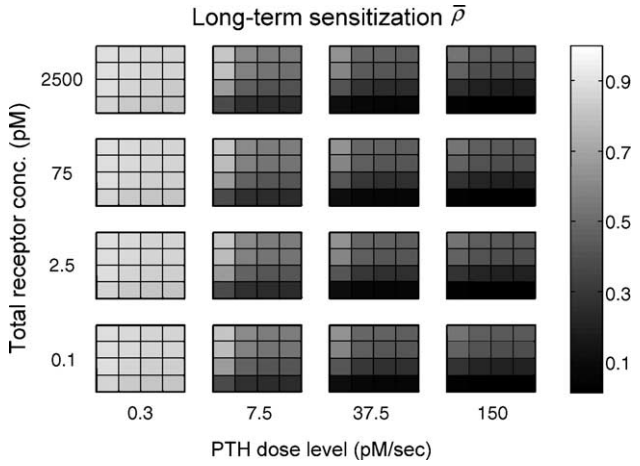

Fig. 7. Long-term sensitization $\bar{\rho}$ for a range of pulsatile dosing patterns as a function of PTH dose level and total receptor concentration. The initial conditions correspond to the sensitized, low-dose continuous state as in Table 2 with the total receptor concentration as given in the graph above. The dosing function (3) was used with $d_{max} = 0.3$, 7.5, 37.5, and 150 pM/s for the following on and off times τ_{on} and τ_{off} : 10 min and 1, 4, 16 h. The resulting long-term sensitizations $\bar{\rho}$ are given in the figure with values corresponding to those given in the colorbar. Each 4 × 4 colored block represents the long-term sensitization over the range of on and off times for the corresponding PTH dose level and total receptor concentration. The model is able to discriminate between different dosing patterns for all receptor concentrations shown here when PTH dose levels are above 0.3 pM/s.

particular physiologic doses of PTH (Fig. 7). As the PTH dose level is varied, the model discriminates continuous from pulsatile dosing for doses larger than 0.3 pM/s, with the best contrast at the 7.5 pM/s dose. It is likely that the 0.3 pM/s dose is not sufficiently large enough to drive the system away from the baseline response seen at 0.015 pM/s. These data suggest that within a range of biologically relevant PTH doses, the two-state model is able to capture the differential behavior of the system for continuous and pulsatile PTH dosing.

The results summarized in Fig. 6 are for continuous and pulsatile dosing patterns with equal C_{max} values (i.e., peak PTH concentration). The model is also able to discriminate between continuous and pulsatile dosing when the total amount of PTH (i.e., the AUC) is equivalent. Simulations were conducted for five different AUC values over 24 h with continuous and pulsatile PTH dosing. As seen in Fig. 8, for the top three dose levels the sensitization state ρ is significantly higher for pulsatile than continuous dosing. These results demonstrate that the model distinguishes continuous from pulsatile dosing when the total PTH dose is equivalent.

The two-state model described here is representative of PTH1R kinetics in vitro, with no endogenous PTH secretion. Since PTH is secreted in a highly pulsatile manner, it is important to determine how the endogenous secretion dynamics may alter the effects of exogenous PTH dosing. This issue was explored using an endogenous dosing function $D_e(t)$ based on PTH secretion data in healthy young women [54]. As seen in Fig. 9, model-simulated endogenous PTH concentrations range between 2.9 and 5 pM, while the

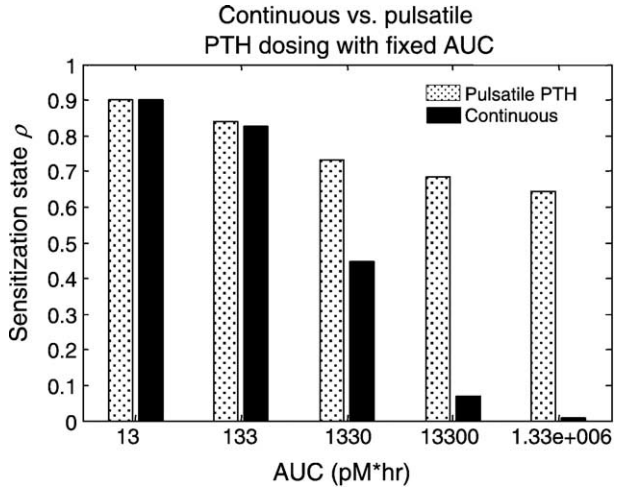

Fig. 8. Comparison of sensitization state ρ for pulsatile and continuous PTH dosing with a fixed AUC (i.e., total cumulative PTH dose). Model simulations started from the sensitized state as in Table 2. The continuous doses had steady-state PTH concentrations of 5.5, 55, 550, and 5500 pM, respectively. For the top three doses, the model clearly discriminates between continuous and pulsatile PTH dosing.

sensitization state ρ exhibits almost no change from the sensitized value of approximately 0.905. This is consistent with other results presented here that demonstrate a similar response to continuous and pulsatile PTH dosing at endogenous PTH levels. Moreover, together these results suggest that the average PTH plasma level following pharmaceutical stimulation of parathyroid secretion may be sufficient to capture the endogenous dynamics of PTH1R [57].

Discussion

A simple, yet biologically plausible mathematical model for parathyroid hormone receptor kinetics can discriminate

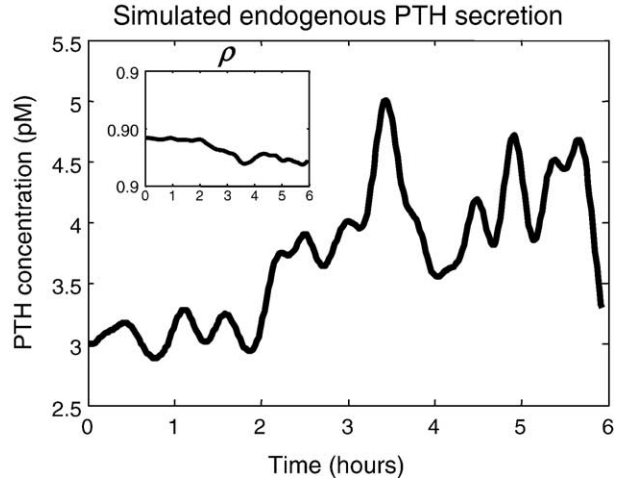

Fig. 9. Model-simulated endogenous PTH secretion and the corresponding system sensitization ρ. PTH secretion data in a healthy young woman were obtained from [54] and incorporated in the model, starting from the fully sensitized state as in Table 2. The pulsatile behavior of PTH did not significantly alter the system sensitization.

between continuous and pulsatile doses of PTH. The model simulations are consistent with numerous experimental and clinical observations suggesting that continuous PTH dosing leads to net bone resorption, whereas pulsatile dosing results in net bone formation.

The ability to discriminate between continuous and pulsatile PTH dosing is critically important since the effects of PTH on the skeleton depend on the particular dosing regimen. When considering PTH1R as a target for new anabolic osteoporosis treatments, it is crucial to have a clear characterization of the action of PTH on bone as a function of dose level and dosing pattern. Moreover, it is important to understand whether the kinetics of PTH1R binding is central to the differential effects of continuous and pulsatile dosing patterns on the skeleton. Based on these studies, it is possible to use this model of PTH1R kinetics to predict the outcomes of different dosing regimens for potential PTH1R agonists.

As demonstrated above, the minimal two-state model (1) is able to predict differential outcomes for different PTH dosing patterns. These simulations are entirely consistent with the hypothesis that the fast kinetics of PTH1R binding plays a role in determining the downstream effects of PTH dosing. Moreover, the modeling results suggest exploring this hypothesis further with new gene expression and proteomic profiling experiments that better detail the short-term signaling cascades responding to continuous vs. pulsatile dosing.

It is important to note that the two-state model does not describe PTH1R-mediated signal transduction since the objective was to determine if PTH1R itself could discriminate between dosing patterns. While both anabolic and catabolic effects of PTH result directly from PTH1R signaling [21,58,59], the two-state model does not explicitly account for the catabolic signaling by PTH since the inactive receptor represents a lack of signaling. One possible interpretation of the model results is that the kinetics of downstream anabolic signaling are parallel to the dynamics of the active complex C_a (and hence able to discriminate pulsatile from continuous dosing), while the catabolic signal cascade is dependent more on the total PTH dose than on the short-term kinetics of C_a.

This issue and the model results presented here further support the development of a more biologically detailed model for evaluating the dynamics of PTH binding and signaling using the two-state model as a core. Based on these findings, it is reasonable to expect that an extended model could be used to predict the effects of different PTH dosing patterns on the stimulation of bone formation. Our current efforts are focused on enhancing this model to accurately describe the biology of PTH1R binding and signaling.

An extended version of the receptor kinetics model will explicitly incorporate receptor-related events involving G proteins, phosphorylation, internalization, and recycling, as well as signal transduction events mediated through the G_s and G_q proteins. This more detailed model will be better compatible with experimental data related to the dynamics of PTH1R, including measurements of desensitization via receptor phosphorylation and internalization. Experimental data such as PTH radioligand binding data, cAMP signaling data, PTH-induced apoptosis data and calcium signaling data will enhance model calibration and accuracy.

The next step after validating the model using PTH as the ligand is to introduce potential therapeutic agents that interact with the PTH1R. Once these compounds are incorporated into the model, the effects of potential PTH mimetics for osteoporosis therapy can be explored. In particular, the model may provide insight into the effects of compounds on bone formation for different dosing frequencies and dose levels, with a goal of designing optimal anabolic strategies for the treatment of postmenopausal osteoporosis.

References

[1] Hock JM, Gera I, Fonseca J, Raisz LG. Human parathyroid hormone-(1–34) increases bone mass in ovariectomized and orchidectomized rats. Endocrinology 1988;122:2899–904.

[2] Finkelstein JS, Hayes A, Hunzelman JL, Wyland JJ, Lee H, Neer RM. The effects of parathyroid hormone, alendronate, or both in men with osteoporosis. N Engl J Med 2003;349:1216–26.

[3] Lindsay R, Nieves J, Formica C, Henneman E, Woelfert L, Shen V, et al. Randomised controlled study of effect of parathyroid hormone on vertebral-bone mass and fracture incidence among postmenopausal women on oestrogen with osteoporosis. Lancet 1997;350:550–5.

[4] Black DM, Greenspan SL, Ensrud KE, Palermo L, McGowan JA, Lang TF, et al. The effects of parathyroid hormone and alendronate alone or in combination in postmenopausal osteoporosis. N Engl J Med 2003;349:1207–15.

[5] Neer RM, Arnaud CD, Zanchetta JR, Prince R, Gaich GA, Reginster JY, et al. Effect of parathyroid hormone (1–34) on fractures and bone mineral density in postmenopausal women with osteoporosis. N Engl J Med 2001;344:1434–41.

[6] Segre GV. Receptors for parathyroid hormone and parathyroid hormone-related protein. In: Bilezikian JP, Raisz LG, Rodan GA, editors. Principles of bone biology. San Diego: Academic Press; 1996. p. 377–403.

[7] Lotinun S, Sibonga JD, Turner RT. Differential effects of intermittent and continuous administration of parathyroid hormone on bone histomorphometry and gene expression. Endocrine 2002;17:29–36.

[8] Blair HC, Athanasou NA. Recent advances in osteoclast biology and pathological bone resorption. Histol Histopathol 2004;19:189–99.

[9] Rubin MR, Cosman F, Lindsay R, Bilezikian JP. The anabolic effects of parathyroid hormone. Osteoporos Int 2002;13:267–77.

[10] Hodsman AB. PTH peptides as anabolic agents in bone. In: Henderson JE, Goltzman D, editors. The osteoporosis primer. Cambridge: Cambridge University Press; 2000. p. 331–46.

[11] Parfitt AM. Parathyroid hormone and periosteal bone expansion. J Bone Miner Res 2002;17:1741–3.

[12] Zhou H, Shen V, Dempster DW, Lindsay R. Continuous parathyroid hormone and estrogen administration increases vertebral cancellous bone volume and cortical width in the estrogen-deficient rat. J Bone Miner Res 2001;16:1300–7.

[13] Dobnig H, Turner RT. Evidence that intermittent treatment with parathyroid hormone increases bone formation in adult rats by activation of bone lining cells. Endocrinology 1995;136:3632–8.

[14] Uzawa T, Hori M, Ejiri S, Ozawa H. Comparison of the effects of

intermittent and continuous administration of human parathyroid hormone(1–34) on rat bone. Bone 1995;16:477–84.
[15] Hock JM, Gera I. Effects of continuous and intermittent administration and inhibition of resorption on the anabolic response of bone to parathyroid hormone. J Bone Miner Res 1992;7:65–72.
[16] Iida-Klein A, Guo J, Xie LY, Juppner H, Potts Jr JT, Kronenberg HM, et al. Truncation of the carboxyl-terminal region of the rat parathyroid hormone (PTH)/PTH-related peptide receptor enhances PTH stimulation of adenylyl cyclase but not phospholipase C. J Biol Chem 1995;270:8458–65.
[17] Qin L, Qiu P, Wang L, Li X, Swarthout JT, Soteropoulos P, et al. Gene expression profiles and transcription factors involved in parathyroid hormone signaling in osteoblasts revealed by microarray and bioinformatics. J Biol Chem 2003;278:19723–31.
[18] Swarthout JT, D'Alonzo RC, Selvamurugan N, Partridge NC. Parathyroid hormone-dependent signaling pathways regulating genes in bone cells. Gene 2002;282:1–17.
[19] Partridge NC, Bloch SR, Pearman AT. Signal transduction pathways mediating parathyroid hormone regulation of osteoblastic gene expression. J Cell Biochem 1994;55:321–7.
[20] Jiang D, Franceschi RT, Boules H, Xiao G. Parathyroid hormone induction of the osteocalcin gene. Requirement for an osteoblast-specific element 1 sequence in the promoter and involvement of multiple-signaling pathways. J Biol Chem 2004;279:5329–37.
[21] Locklin RM, Khosla S, Turner RT, Riggs BL. Mediators of the biphasic responses of bone to intermittent and continuously administered parathyroid hormone. J Cell Biochem 2003;89:180–90.
[22] Qin L, Raggatt LJ, Partridge NC. Parathyroid hormone: a double-edged sword for bone metabolism. Trends Endocrinol Metab 2004;15:60–5.
[23] Bisello A, Chorev M, Rosenblatt M, Monticelli L, Mierke DF, Ferrari SL. Selective ligand-induced stabilization of active and desensitized parathyroid hormone type 1 receptor conformations. J Biol Chem 2002;277:38524–30.
[24] Kroll MH. Parathyroid hormone temporal effects on bone formation and resorption. Bull Math Biol 2000;62:163–88.
[25] Rattanakul C, Lenbury Y, Krishnamara N, Wollkind DJ. Modeling of bone formation and resorption mediated by parathyroid hormone: response to estrogen/PTH therapy. Biosystems 2003;70:55–72.
[26] Lemaire V, Tobin FL, Greller LD, Cho CR, Suva LJ. Modeling the interactions between osteoblast and osteoclast activities in bone remodeling. J Theor Biol 2004;229:293–309.
[27] Segel LA, Goldbeter A, Devreotes PN, Knox BE. A mechanism for exact sensory adaptation based on receptor modification. J Theor Biol 1986;120:151–79.
[28] Parfitt AM. Targeted and nontargeted bone remodeling: relationship to basic multicellular unit origination and progression. Bone 2002;30:5–7.
[29] Fitzpatrick LA, Bilezikian JP. Actions of parathyroid hormone. In: Bilezikian JP, Raisz LG, Rodan GA, editors. Principles of bone biology. San Diego: Academic Press; 1996. p. 339–46.
[30] Pun KK, Ho PW, Nissenson RA, Arnaud CD. Desensitization of parathyroid hormone receptors on cultured bone cells. J Bone Miner Res 1990;5:1193–200.
[31] Spurney RF, Flannery PJ, Garner SC, Athirakul K, Liu S, Guilak F, et al. Anabolic effects of a G protein-coupled receptor kinase inhibitor expressed in osteoblasts. J Clin Invest 2002;109:1361–71.
[32] Dicker F, Quitterer U, Winstel R, Honold K, Lohse MJ. Phosphorylation-independent inhibition of parathyroid hormone receptor signaling by G protein-coupled receptor kinases. Proc Natl Acad Sci U S A 1999;96:5476–81.
[33] Conway BR, Minor LK, Xu JZ, D'Andrea MR, Ghosh RN, Demarest KT. Quantitative analysis of agonist-dependent parathyroid hormone receptor trafficking in whole cells using a functional green fluorescent protein conjugate. J Cell Physiol 2001;189:341–55.
[34] Bergwitz C, Abou-Samra AB, Hesch RD, Juppner H. Rapid desensitization of parathyroid hormone dependent adenylate cyclase in perifused human osteosarcoma cells (SaOS-2). Biochim Biophys Acta 1994;1222:447–56.
[35] Tawfeek HA, Che J, Qian F, Abou-Samra AB. Parathyroid hormone receptor internalization is independent of protein kinase A and phospholipase C activation. Am J Physiol: Endocrinol Metab 2001;281:E545–57.
[36] Lauffenburger DA, Linderman JJ. Receptors: models for binding, trafficking, and signaling. New York: Oxford University Press; 1993.
[37] Weiss JM, Morgan PH, Lutz MW, Kenakin TP. The cubic ternary complex receptor-occupancy model: I. Model description. J Theor Biol 1996;178:151–67.
[38] Schwartz TW, Holst B. Molecular structure and function of 7TM G-protein-coupled receptors. In: Foreman JC, Johansen T, editors. Textbook of receptor pharmacology. Boca Raton: CRC Press; 2003. p. 81–109.
[39] Waelbroeck M. Kinetics versus equilibrium: the importance of GTP in GPCR activation. Trends Pharmacol Sci 1999;20:477–81.
[40] Gardella TJ, Juppner H. Molecular properties of the PTH/PTHrP receptor. Trends Endocrinol Metab 2001;12:210–7.
[41] Leff P. The two-state model of receptor activation. Trends Pharmacol Sci 1995;16:89–97.
[42] Trzeciakowski JP. Stimulus amplification, efficacy, and the operational model. Part II—Ternary complex occupancy mechanisms. J Theor Biol 1999;198:347–74.
[43] Pierce KL, Premont RT, Lefkowitz RJ. Seven-transmembrane receptors. Nat Rev, Mol Cell Biol 2002;3:639–50.
[44] Goldbeter A. Biochemical oscillations and cellular rhythms: the molecular bases of periodic and chaotic behaviour. Cambridge: Cambridge University Press; 1996.
[45] Lauffenburger DA, Linderman JJ. Receptors: models for binding, trafficking, and signaling. New York: Oxford University Press; 1993.
[46] Abou-Samra AB, Jueppner H, Potts Jr JT, Segre GV. Inactivation of pertussis toxin-sensitive guanyl nucleotide-binding proteins increase parathyroid hormone receptors and reverse agonist-induced receptor down-regulation in ROS 17/2.8 cells. Endocrinology 1989;125:2594–9.
[47] Yamamoto I, Shigeno C, Potts Jr JT, Segre GV. Characterization and agonist-induced down-regulation of parathyroid hormone receptors in clonal rat osteosarcoma cells. Endocrinology 1988;122:1208–17.
[48] Guo J, Iida-Klein A, Huang X, Abou-Samra AB, Segre GV, Bringhurst FR. Parathyroid hormone (PTH)/PTH-related peptide receptor density modulates activation of phospholipase C and phosphate transport by PTH in LLC-PK1 cells. Endocrinology 1995;136:3884–91.
[49] Riccobene TA, Omann GM, Linderman JJ. Modeling activation and desensitization of G-protein coupled receptors provides insight into ligand efficacy. J Theor Biol 1999;200:207–22.
[50] Hoare SR, Gardella TJ, Usdin TB. Evaluating the signal transduction mechanism of the parathyroid hormone 1 receptor. Effect of receptor-G-protein interaction on the ligand binding mechanism and receptor conformation. J Biol Chem 2001;276:7741–53.
[51] Schmitt CP, Schaefer F, Bruch A, Veldhuis JD, Schmidt-Gayk H, Stein G, et al. Control of pulsatile and tonic parathyroid hormone secretion by ionized calcium. J Clin Endocrinol Metab 1996;81:4236–43.
[52] Schmitt CP, Huber D, Mehls O, Maiwald J, Stein G, Veldhuis JD, et al. Altered instantaneous and calcium-modulated oscillatory PTH secretion patterns in patients with secondary hyperparathyroidism. J Am Soc Nephrol 1998;9:1832–44.
[53] Rodan SB, Wesolowski G, Ianacone J, Thiede MA, Rodan GA. Production of parathyroid hormone-like peptide in a human osteosarcoma cell line: stimulation by phorbol esters and epidermal growth factor. J Endocrinol 1989;122:219–27.
[54] Samuels MH, Veldhuis J, Cawley C, Urban RJ, Luther M, Bauer R, et al. Pulsatile secretion of parathyroid hormone in normal young subjects: assessment by deconvolution analysis. J Clin Endocrinol Metab 1993;77:399–403.
[55] Shampine L, Reichelt M. The MATLAB ODE suite. SIAM J Sci Comput 1997;18:1–22.

[56] Peck WA, Kohler G. Hormonal and nonhormonal desensitization in isolated bone cells. Calcif Tissue Int 1980;32:95–103.
[57] Gowen M, Stroup GB, Dodds RA, James IE, Votta BJ, Smith BR, et al. Antagonizing the parathyroid calcium receptor stimulates parathyroid hormone secretion and bone formation in osteopenic rats. J Clin Invest 2000;105:1595–604.
[58] Jilka RL, Weinstein RS, Bellido T, Roberson P, Parfitt AM, Manolagas SC. Increased bone formation by prevention of osteoblast apoptosis with parathyroid hormone. J Clin Invest 1999;104:439–46.
[59] Nishida S, Yamaguchi A, Tanizawa T, Endo N, Mashiba T, Uchiyama Y, et al. Increased bone formation by intermittent parathyroid hormone administration is due to the stimulation of proliferation and differentiation of osteoprogenitor cells in bone marrow. Bone 1994;15:717–23.